JBC Papers in Press. Published on May 19, 2019 as Manuscript RA119.007983
The latest version is at http://www.jbc.org/cgi/doi/10.1074/jbc.RA119.007983

Proline mediates metabolic communication between retinal pigment epithelial cells and the retina

Michelle Yam[1,2] , Abbi L Engel[3], Yekai Wang[1,2], Siyan Zhu[1,2], Allison Hauer[1,2], Rui Zhang[1,4], Daniel Lohner[1,2], Jiancheng Huang[1,5,6], Marlee Dinterman[1,2], Chen Zhao[5], Jennifer R. Chao[3*] and Jianhai Du[1,2*]

Running title: *Proline metabolism in RPE and retina*

[1]Department of Ophthalmology, West Virginia University, Morgantown, WV 26506

[2]Department of Biochemistry, West Virginia University, Morgantown, WV 26506

[3]Department of Ophthalmology, University of Washington, Seattle, WA 98109

[4]Save Sight Institute, University of Sydney, 8 Macquarie Street, Sydney, NSW 2000, Australia

[5] Eye Institute, Institute, Eye & ENT Hospital, Shanghai Medical College, Fudan University, Shanghai 200031, China

[6]Department of Ophthalmology, The First Affiliated Hospital of Nanjing Medical University, State Key Laboratory of Reproductive Medicine, Nanjing, China

* Corresponding Authors: Jennifer R. Chao, 750 Republican Street, Box 358058, Seattle WA 98109; Phone: (206) 221-0594; Email: jrchao@uw.edu; or Jianhai Du, One Medical Center Dr, PO Box 9193, WVU Eye Institute, Morgantown, WV 26505; Phone: (304)-598-6903; Fax: (304)-598-6928; Email: jianhai.du@wvumedicine.org.

Keywords: proline; retinal pigment epithelium; retina; mitochondrial metabolism; age-related macular degeneration (AMD); oxidative stress; visual function; glucose metabolism;

ABSTRACT

The retinal pigment epithelium (RPE) is a monolayer of pigmented cells between the choroid and the retina. RPE dysfunction underlies many retinal degenerative diseases, including age-related macular degeneration, the leading cause of age-related blindness. To perform its various functions in nutrient transport, phagocytosis of the outer segment, and cytokine secretion, the RPE relies on an active energy metabolism. We previously reported that human RPE cells prefer proline as a nutrient and transport proline-derived metabolites to the apical, or retinal, side. In this study, we investigated how RPE utilizes proline *in vivo* and why proline is a preferred substrate. By using ^{13}C proline labeling both *ex vivo* and *in vivo*, we found that the retina rarely uses proline directly, whereas the RPE utilizes it at a high rate, exporting proline-derived mitochondrial intermediates for use by the retina. We observed that in primary human RPE cell culture, proline is the only amino acid whose uptake increases with cellular maturity. In human RPE, proline was sufficient to stimulate *de novo* serine synthesis, increase reductive carboxylation, and protect against oxidative damage. Blocking proline catabolism in RPE impaired glucose metabolism and glutathione production. Notably, in an acute model of RPE-induced retinal degeneration, dietary proline improved visual function. In conclusion, proline is an important nutrient that

supports RPE metabolism and the metabolic demand of the retina.

The retinal pigment epithelium (RPE) is a monolayer of pigmented cells between the choroid and the retina. RPE dysfunction contributes to the pathogenesis of many retinal degenerative diseases, including age-related macular degeneration (AMD), the leading cause of blindness in the older population. In order to maintain its functions in nutrient transport, phagocytosis of outer segment and cytokine secretion, the RPE relies on an active energy metabolism. We reported recently that the RPE has a high capacity for reductive carboxylation, a reverse tricarboxylic acid (TCA) cycle (1). Using an unbiased metabolomics screen, we found that RPE heavily consumes proline to fuel both mitochondrial oxidative phosphorylation and reductive carboxylation (2).

Proline has diverse functions in different organisms (3-5). Proline is well known to accumulate in plants to combat various environmental stressors (6,7). Proline is also a significant component (up to 25%) of collagen, which is the most abundant protein in extracellular matrix (ECM) such as the Bruch's membrane located underneath RPE cells (3). Proline can be catabolized through proline dehydrogenase (PRODH) to donate electrons directly to ubiquinone or into glutamate to enter the mitochondrial TCA cycle (2,4,8,9). In several invertebrates, proline is the major energy source (9). In worms, proline supplementation extends their lifespans, (10) and a mutation that shifts their metabolism towards proline catabolism increases their lifespans more than two fold (11,12).

Proline is not an essential amino acid. It can be produced from glutamate through pyrroline-5-carboxylate synthase (P5CS), from collagen degradation through prolidase, or from ornithine through ornithine aminotransferase (OAT). Inborn errors of genes in proline metabolism can result in retinal degeneration. A mutation in the gene encoding P5CS has been associated with retinitis pigmentosa (13). Mutations in OAT are well-documented to cause gyrate atrophy, characterized by lobular loss of the RPE/choroid and progressive retinal degeneration (14-16). OAT deficiency results in accumulation of more than 10 fold levels of ornithine in the plasma and ornithine can inhibit P5CS *in vitro* (17). In RPE cell lines, supplementation of proline has been shown to rescue ornithine cytotoxicity (18,19). A proline transporter solute carrier family 6, member 20 (SLC6A20) has been regarded as a RPE signature gene (20-22), and it is one of 22 RPE genes shared by both human and mouse RPE (20). Recent large-scale genome-wide association study (GWAS) reports that the locus of this proline transporter is significantly associated with AMD (22,23). Overall, previous findings implicate proline metabolism as a potentially essential component of RPE health and function.

In this report, we investigate how proline is utilized by the RPE and retina as well as the functional roles of proline consumption. By using ^{13}C tracing, we found that proline fuels RPE mitochondrial metabolism. The RPE also exports proline-derived intermediates to the retina *ex vivo* and *in vivo*. As RPE cells mature *in vitro*, they become more dependent on proline as a nutrient substrate. Proline supplementation confers resistance against oxidative damage and improves visual function.

Results

Mouse RPE/choroid but not retina utilizes proline ex vivo and exports proline-derived intermediates.

We previously reported that human fetal RPE (hRPE) in culture consumes more proline than other amino acids (2). To investigate whether native RPE utilizes proline, we isolated mouse RPE/choroid and retina and incubated them with ^{13}C labeled proline (**Fig 1A**). We did not isolate the RPE from the choroid as separation could disrupt RPE metabolism and influence cell viability. We found that the RPE/choroid

complex consumed proline >100X faster than the retina (**Fig 1B**). This finding supports our previous reports that glucose and glutamine are major fuels for retinal mitochondrial metabolism (24). Proline can be metabolized into mitochondrial intermediates through PRODH. After incubation with ^{13}C proline, we found a high percentage of labeled TCA cycle intermediates (20-30%), with the exception of succinate, in total pools in the RPE/choroid. This is in contrast to only 2% of labeled intermediates in the retina (**Fig 1C-I**), confirming that proline might be a major nutrient for RPE. ^{13}C proline could generate α-ketoglutarate (αKG) for either the TCA cycle to produce M4 citrate or reductive carboxylation to produce M5 citrate (**Fig S1A**)(2). We found M5 citrate in the RPE/choroid but not retina, indicating that reductive carboxylation is active in native RPE cells (**Fig S1B-C**). Additionally, we found ~2% of M3 pyruvate and ~0.5% of M3 PEP labeled by ^{13}C proline, which should be generated mostly through malic enzyme rather than phosphoenolpyruvate carboxykinase (PEPCK) (**Fig S1A, D**). To study whether RPE can release proline-derived intermediates, we measured the incubation media and found that ^{13}C labeled intermediates increased in a time-dependent fashion in RPE/choroid cultures (**Fig 1J-L**).

RPE utilizes proline to fuel retinal metabolism in vivo.

To study proline metabolism *in vivo*, we performed hyperinsulinemic-euglycemic clamp in conscious, unrestrained mice and infused ^{13}C proline through the jugular vein continuously for 4 hours (hrs) (25). Blood from the carotid artery was sampled at different time points to monitor ^{13}C proline labeling in the plasma, and the RPE/choroid and retina were collected quickly after the 4 hr infusion (**Fig 2A**). We infused at 2 mg/kg/min and 4 mg/kg/min based on the concentration of proline in the plasma relative to glutamine. Plasma glutamine is slightly higher than proline and glutamine is infused at 2 mg/kg/min in the literature (26). Both doses of proline rapidly replaced 60-80% of endogenous proline and reached a steady state within 30 minutes (**Fig 2B**). ^{13}C labeled proline is about 3-4 fold higher in the RPE/choroid than retina (**Fig 2C**). To study the flow of proline-derived intermediates from RPE to retina, we analyzed the labeled patterns in the intermediates. Five carbon labeled ^{13}C (M5) proline can be converted into M5 glutamate and M5 αKG to enter TCA cycle. In the first turn, one carbon will be lost as CO_2 through αKG dehydrogenase to generate M4 intermediates (**Fig 2D-E**). More carbons will be lost in the second and third turn. Interestingly, M5 glutamate, M5 αKG and M4 mitochondrial intermediates were much higher in RPE/choroid than retina (**Fig 2F**), while M1 intermediates were much higher in the retina than RPE/choroid (**Fig 2G**). These results further support our hypothesis that RPE utilizes proline to form mitochondrial intermediates which are then exported to fuel retinal mitochondria (**Fig 2E**).

Human RPE cell switches to proline utilization during RPE maturation.

Depending on culture conditions, hRPE can take 4-6 weeks to mature, forming their characteristic cobble stone hexagonal morphology, pigmentation and expression of typical RPE markers (**Fig 3A-D**). To study proline consumption during RPE maturation, we sampled media 24 hrs after media change in hRPE culture at weeks 1-4 and measured the metabolites by gas chromatography–mass spectrometry (GC MS) (**Fig 3A-E**). Week 0 (W0) consisted of the control media incubated for 24 hrs without hRPE cells. Proline was the only amino acid whose consumption increased with RPE maturation. Proline was almost undetectable in W3 and W4 media (**Fig 3E**), consistent with our previous report that RPE consumes a large amount of proline (2). W4 hRPE consumed most other amino acids at a similar rate to W1 hRPE, with the exception of alanine, glutamine, glutamate and taurine. To confirm this finding, we measured the nutrient consumption at the same time plated at different densities. After culture for one week, the hRPE with higher initial plating densities were noted to mature quickly

than those plated at lower densities (**Fig S2A-C**). As expected, proline was the only amino acid that was consumed in a density/maturity-dependent manner, suggesting that RPE cells increase their proline consumption with cellular maturity (**Fig 3F**). Consistently, both mature hRPE and induced pluripotent stem (iPS) cells-derived RPE demonstrated high proline consumption while RPE cell lines, ARPE-19 and hRPE-1 cells, and human kidney epithelial cell line HEK 293T cells used either much less proline or none at all (**Fig 3G**).

Inhibition of PRODH partially blocks RPE proline consumption and disrupts glucose and amino acid metabolism.

To determine the pathway responsible for high proline uptake in RPE, we used inhibitors to block several known pathways in proline catabolism including tetrahydro-2-furoic acid (T2FA), canaline, halofuginone (HF) and 1,4-dihydrophenonthrolin-4-one-3-Carboxylic acid (DPCA) (**Fig 4A**). These inhibitors block proline dehydrogenase (PRODH), OAT, prolyl-tRNA synthetase (PRS) and prolyl-4-hydroxylase (P4H) to inhibit proline catabolism into glutamate, ornithine, L-prolyl-tRNAPro in protein synthesis and 4 -hydroxyproline (4-OH Pro) in collagen, respectively. (27-30). After 48 hrs in RPE media (containing 0.447 mM proline), 95% of proline was used (**Fig 4B**). With the exception of T2FA, all other inhibitors could not block proline consumption, supporting our previous finding that proline is partly metabolized into glutamate for mitochondrial metabolism (**Fig 4C**). To study the impact of PRODH on the consumption of other nutrients and cell metabolism, we quantified key metabolites in glucose and amino acid metabolism (**Table S1**) by LC MS/MS and GC MS in the media and the cell supernatant with T2FA treatment. In addition to proline, inhibition of PRODH resulted in significant accumulation of glucose in both RPE media and RPE cells (**Fig 4D-E**). Consistently, glucose-derived intermediates including lactate, alanine, dihydroxyacetone phosphate (DHAP), glyceraldehyde 3-phosphate (G3P), and serine were substantially decreased in media and/or cells (**Fig 4D-E**). Purine metabolites are sensitive to the availability of glucose in RPE (31). As expected, xanthine, guanosine and inosine dramatically increased in RPE cells (**Fig 4E**). Additionally, inhibition of PRODH decreased many mitochondrial intermediates, glutathione (GSH), glutamine, and increased branch-chain amino acids. These data suggest that proline metabolism may be critical for glucose metabolism and utilization of other amino acids.

Proline stimulates de novo serine/glycine synthesis, glycolysis and mitochondrial metabolism.

To further examine the impact of proline on glucose metabolism, we incubated RPE cells with or without 1 mM proline in the presence of ^{13}C glucose (**Fig 5A**) and analyzed metabolites in both media and cells (**Fig 5B-C**). ~85% of proline in the media was used by 24 hrs and almost of all proline was consumed by 48 hrs (**Fig 5A**). The addition of proline reduced the percentage of ^{13}C labeled mitochondrial TCA intermediates in the media and cells (**Fig 5B-C**, **Fig S3**). The labeling pattern (isotopologue) showed that M2 metabolites (derived from first turn of the TCA cycle) remained unchanged, but M4 (derived from the second turn of the TCA cycle), M3 and M1 (derived from pyruvate carboxylase or multiple turns of the TCA cycle) intermediates were decreased (**Fig S4-5**). These results indicate that mitochondria have a preference for utilizing proline rather than glucose as a substrate for four carbon pools. Surprisingly, proline increased the flux of serine and glycine from ^{13}C glucose (**Fig 5B-C, Fig S3**). While the abundance (concentration or pool size) of labeled serine and glycine was significantly increased, the unlabeled serine and glycine were not (**Fig 5D-E, Fig S6**) confirming that proline stimulates *de novo* serine biosynthesis from glucose. Additionally, proline increased ^{13}C lactate, ^{13}C pyruvate and ^{13}C alanine in media and cells (**Fig 5C-E**) and increased the overall concentration of aspartate, glutamate and

glutamine in RPE (**Fig 5 E**, **Fig S6)**. These results suggest that proline enhances glycolysis and synergizes with glucose metabolism. To further examine whether proline enhances mitochondrial energy metabolism, we measured mitochondrial O_2 consumption using an Extracellular Flux Analyzer. Proline doubled the maximum O_2 consumption comparable to glucose alone (**Fig S7**). This is comparable to the combined effect of pyruvate and glutamine.

Proline protects RPE cells from oxidative damage.

To test whether proline protects against oxidative damage in RPE, we incubated hRPE cells with proline in the presence of 1 mM hydrogen peroxide. Cell death was assessed by quantifying ethidium homodimer (EthD) staining of dead cells, lactate dehydrogenase (LDH) activity assay in the culture media, and bright-field imaging of morphological changes. There was no difference in cell death in control hRPE with or without the addition of proline within 48 hrs. Hydrogen peroxide treatment increased EthD-positive cells, accumulated LDH in the media and decreased cell density (**Fig 6A-D**). Supplementation with proline significantly reduced the number of dead cells and decreased LDH activity compared to hydrogen peroxide treatment alone (**Fig 6A-D**). To understand the mechanism for this protection, we analyzed metabolites in the cell media. Hydrogen peroxide increased DHAP and GAP but decreased downstream lactate and pyruvate (**Fig 6E-F**), consistent with our previous report that oxidative stress blocks glyceraldehyde 3-phosphate dehydrogenase (GAPDH) in glycolysis (1). Proline decreased DHAP and GAP, and offset the reduction of downstream metabolites including lactate, pyruvate, alanine and glutamate and glutamine, confirming our finding that proline is important for glucose metabolism.

Proline-enriched diet improves visual function after induced oxidative damage to the RPE.

To study whether proline can reduce oxidative damage *in vivo*, we fed mice with a customized high proline (High-Pro) diet or regular amino acid diet for two weeks. Although the total amount of calories in the diets were similar, the High-Pro diet consisted of 2% proline (5.7 times higher proline compared to the regular amino acid diet) (**Table S2**). We then injected the mice with sodium iodate (SI), which selectively damages the RPE and induces retinal degeneration (32,33). Mice had similar body weight and food intake between the regular diet and High-Pro diet (**Fig S8**).The High-Pro diet increased plasma proline approximately 2 fold over the regular diet in mice (**Fig 7A**). In the electroretinogram (ERG) testing, there was no difference in both the scotopic and photopic responses between the regular diet and High-Pro diet at baseline (**Fig 7B-F**). We did not quantify photopic a-wave since the response was small with more variations. As expected, SI treatment attenuated ERG responses. However, the High-Pro diet protected the decreased a-wave amplitudes and b-wave amplitudes (**Fig 7B-F**), suggesting that proline improves both rod and cone function. Furthermore, we examined glial cell activation by immunostaining with glial fibrillary acidic protein (GFAP) (**Fig S9**). SI caused massive staining of GFAP to activate glia, but High-Pro reduced this activation (**Fig S9**). To test the effect on photoreceptor viability, we stained cone photoreceptors with peanut agglutinin (PNA) in flat mount retinas. The High-Pro diet showed protection against the photoreceptor damage caused by SI treatment (**Fig 8A-B**). These results suggest that a proline-enriched diet is sufficient to improve acute retinal damage in SI-treated mice.

Discussion

The RPE has easy access to different nutrients to support its active metabolism and to meet the energetic demand of the outer retina. However, how the RPE utilizes these nutrients and shares them with the retina is still unclear. In this study, we report that proline is an important substrate for both RPE metabolism and its metabolic communication with the retina (**Fig 9**).

Proline regulates glucose metabolism and can protect the RPE from oxidative damage.

Why do cells consume large amounts of free proline? A recent study examining the proteomes of bacteria, basal eukaryotes, and animals reveals that the demand for free proline increased with the emergence of animals. This may be necessary, as multi-cellular organisms require the production proline-rich proteins such as collagens. The consumption of proline may also avoid the depletion of glutamate, as there is a conserved evolution of a fusion protein of glutamyl-tRNA synthetase and proly-tRPNA synthetase (34). We have found that proline increases glutamate and glutamine content in RPE. Glutamate and its products in the TCA cycle, such as αKG, can be exported to support outer retinal metabolism *in vitro* (2) and *in vivo*. The oxidation of proline may allow maximal flux through the TCA cycle in the oxidation of glucose and ensure a steady supply of these important intermediates in both the RPE and retina. RPE is active in synthesizing ECM, including different types of collagens, and exports them to maintain Bruch's membrane (35,36). Radioactive-labeled proline was readily incorporated into collagen in feline and primate RPE cells (37,38). The ECM remodeling occurs in both early and advanced AMD, simultaneously with RPE metabolic dysfunction (35,39,40). Proline metabolism provides a link between ECM remodeling and mitochondrial metabolism. It remains to be determined how cells balance the distribution of proline for collagen synthesis and catabolism in healthy and diseased RPE.

Proline is an efficient mitochondrial fuel. In fly muscles, partial oxidation of proline generates 0.52 mol ATP/g, which is only slightly lower than that of lipids (0.65 mol ATP/g) but much higher than glucose (0.18 ATP/g) (41). Besides oxidizing proline to generate NADH, PRODH is a flavin-dependent enzyme that is capable of using FAD as a co-factor to drive ATP synthesis (42). This is consistent with our data demonstrating that proline elicits higher maximal O_2 in RPE cells. Interestingly, a recent study reveals that RPE has much higher FAD levels than retina (43). In breast cancer cells, mitochondrial metabolism is shifted to proline catabolism to support their growth and form lung metastases (44). We found that hRPE increasingly rely upon proline consumption in culture. Proline may efficiently fuel mitochondrial metabolism to meet the high metabolic demand during maturation. To control cellular growth and division, a metabolic switch from glycolysis to mitochondrial oxidative phosphorylation (OXPHOS) is a common feature during terminal differentiation (45,46). Mitochondrial mass and OXPHOS genes are significantly increased during RPE maturation (47). Inhibition of mitochondrial OXOPHOS decreases RPE maturation resulting in RPE dedifferentiation (48). Additionally, we found that proline increases pyruvate in both media and cells. Pyruvate has been reported to stimulate RPE differentiation and pigmentation in culture (49).

It is surprising that proline enhances serine *de novo* synthesis through glucose. Serine can be synthesized from the glycolytic intermediate 3-phosphoglycerate (3PG), which involves three enzymes, phosphoglycerate dehydrogenase (PHGDH), phosphoserine aminotransaminase (PSAT) and phosphoserine phosphatase (PSPH). We did not find any difference in 3PG, indicating increased flux of the latter two enzymes. PSAT catalyzes the conversion of 3-phosphohydroxypyruvate and glutamate to 3-phosphoserine and αKG (**Fig 9)**. Transamination from glutamate to ketoacid is a common reaction to generate αKG and non-essential amino acids. The increase of glutamate by proline most probably stimulates the transamination reaction of PSAT to increase serine and glycine biosynthesis. Consistently, in a transcriptome database of human RPE/choroid and retina, PSAT transcripts were 30-fold higher than alanine transaminase and 2-fold higher than cytosolic aspartate transaminase (50). Interestingly, glutamine-derived glutamate contributes to PSAT activity to generate αKG,

which regulates embryonic stem cell differentiation (51). We reported previously that co-culturing retina with RPE dramatically increases serine and glycine in the retina (2). A pharmacological study has also indicated retinal glycine content comes from transport rather than *de novo* synthesis in retinal neurons (52). The serine biosynthesis pathway is tightly linked with the synthesis of phospholipids, the generation of glycine, cysteine, glutathione and NADPH, and donation of one-carbon unit (53). The retina has been found to have a higher rate of serine incorporation in phospholipids (53) . Glycine and cysteine are substrates used to synthesize glutathione, an important antioxidant. We found that the inhibition of proline catabolism decreases both serine and glutathione in RPE. Glycine also makes up one third of collagen and serine *de novo* pathway regulates TGF β-mediated collagen synthesis in pulmonary fibrosis (20,54). The transcripts of PHGDH and PSAT are approximately 6 fold higher in RPE/choroid than retina (50), which supports our finding that the RPE may be the major site of serine and glycine synthesis. Proline enhances this pathway to maintain the active metabolism of the outer retina.

How proline protects oxidative damage in RPE cells? NADPH is needed for reduced glutathione to remove reactive oxygen species and manage oxidative stress (55). Major sources of NADPH include the pentose phosphate pathway (PPP), serine-driven one-carbon metabolism, malic enzyme and NADP-dependent isocitrate dehydrogenases (IDH) (56,57). In cancer cells, serine-driven NADPH is comparable to the PPP (56). IDH provides a substantial amount of NADPH in rod photoreceptors (58). The protozoan parasite, *Trypanosoma brucei*, adapts to its hosts' environment and relies on proline as a carbon source. Malic enzyme and PPP are two major pathways used by this parasite to generate NADPH through proline to combat oxidative stress (59). In human RPE, we reported that reductive carboxylation through IDH confers RPE to resist against oxidative damage (1). Our data showed that proline stimulates the serine pathway, increases the malic enzyme pathway to generate pyruvate, and enhances reductive carboxylation in RPE **(Fig 9)**. Furthermore, inhibition of proline oxidation inhibits serine synthesis and reduces the level of glutathione (**Fig 4**). The activation of the pathways for NADPH production may contribute to the ability of proline to protect against oxidative damage.

Proline is a non-essential amino acid but 10–115 mg/liter of proline is included in most of the widely used protocols for human RPE culture media (60-62). Our data suggest that proline may be critical for RPE maturation and retinal function. To our knowledge, there are 5 known proline transporters (SLC6A20, SLC6A7, SLC3A1, SLC36A2, SLC36A4). We analyzed a transcriptional database for maturation and differentiation of human RPE culture (63). Only SLC6A20 is significantly upregulated in matured and differentiated RPE cells (**Fig S10**). SLC6A20, a Na^+ and Cl^- dependent proline transporter, is highly enriched in human RPE and mouse RPE (20-22). Further study should elucidate the importance of this transporter in proline metabolism, the synthesis of proline-rich proteins and RPE function.

One important finding in this study is that RPE utilizes proline to generate mitochondrial intermediates for outer retina. To maintain visual function and high turnover of outer segments, the retina has an extremely active metabolism (64). Glycolysis and mitochondrial oxidative phosphorylation are two primary pathways for energy metabolism. Like tumors, retinas prefer aerobic glycolysis, also called Warburg effect, converting most of glucose into lactate rather than into mitochondrial intermediates (24,64). However, retina also has active oxidative phosphorylation in its mitochondria packed in the ellipsoid (64). The proline-derived intermediates may provide substrates to retinal mitochondria for ATP synthesis and generation of neurotransmitters. Consistently, high proline diet improves visual function and increases photoreceptor survival in

an acute model of retinal degeneration. We found proline protects both rod and cone responses, but scotopic a-wave is better preserved than b-wave. The a-wave reflects the hyperpolarization of the photoreceptors due to closure of sodium ion channels in the outer-segment membrane and the b-wave originates from photoreceptor-driven bipolar cells induced by neurotransmitter glutamate and the change of potassium (65,66). It is reported that sodium iodate could directly cause synaptic damage to diminish b-wave (67). Additionally, Müller glial cells also significantly contribute to b-wave by regulating the biosynthesis of glutamate and extracellular potassium concentration (64,65). Our data found that proline could only partially reduce the glial activation by sodium iodate (Fig S9). Future investigation of the protection by proline *in vivo* including dose, longitude and other models of retinal degenerations will yield important information for potential treatment with proline supplementation.

In conclusion, we provide evidence that proline is an important nutrient for RPE. The ability to utilize proline may promote RPE maturation, regulate glucose metabolism, increase the capacity of RPE to defend against oxidative stress, and allow for the export of critical intermediates for utilization by the outer retina.

Experimental Procedures

All the reagents, animals and key resources were detailed in the key resources form (**Table S3**).

Cell culture

Human fetal RPE cells were isolated and primarily cultured as described previously (2,68). The protocol is approved by the University of Washington Institutional Review Board. All procedures conform to the ethical principles outlined in the Declaration of Helsinki. RPE cells were plated in 12-well or 24-well plates in RPE medium consisting of MEM α medium, non-essential amino acids (NEAA), N1 supplement, 1% (Vol/Vol) FBS, taurine, hydrocortisone and triodo-thryonine and penicillin-streptomycin. The cells were changed into fresh medium 24 or 48 hrs before harvesting media for metabolite analysis. For proline supplementation and hydrogen peroxide experiment, the RPE cells were changed into clear DMEM with 5.5 mM glucose and 1% (Vol/Vol) FBS. iPS cells were differentiated to RPE using the speed differentiation protocol developed by Buchholz et al 2013(69). RPE cells were either manually picked or trypsinized, depending on the quality of differentiation. The RPE was then plated on Matrigel® Matrix and cultured as described previously in an RPE medium containing 5% FBS and 10uM ROCK inhibitor (Y-27632 dihydrochloride, Tocris Bioscience). After reaching confluency, the FBS concentration in the media was decreased to 1% and ROCK inhibitor was no longer added to the media. hRPE and iPSC RPE cells were plated at 0.25 million cells in a 24-well plate, 0.5 million cells for 12-well plates and 0.8 million cells for 6 well plates. A-RPE 19, hRPE1 and HEK 293 T cells were plated seeded at 0.8 million cells/per well in 6-well plate and grown for a week in DMEM/F12 medium supplemented with NEAA and 5% (Vol/Vol) FBS.

Cell death staining

The cell death staining was performed as reported previously (1). RPE cells were grown for 4–5 weeks in 24-well plates and treated with 1mM H_2O_2 with or without 1 mM pyruvate in DMEM. Media was removed and replaced with 500 μL KRB and EthD dye. Bright field and fluorescent images were taken with the Evos digital inverted microscope (AMG) and counted using Fiji or Image J software.

LDH activity assay

Culture media (20 μL) was incubated with enzyme assay mix as described (1). The change of absorbance (340 nM) over time was read by a microplate reader.

Metabolite analysis

The metabolites harvested from retinal explants and human RPE were analyzed with GC MS or LC MS as we described in details before (31,70). For medium metabolites, 10 μl of medium or plasma was mixed with 40 μl cold methanol to extract metabolites for analysis with GC MS or LC MS. The intracellular metabolites were extracted by using 80% cold methanol. One mouse retina or RPE/choroid was snap-frozen in liquid nitrogen and homogenized with 80% cold methanol to extract metabolites. For GC MS, the samples were derivatized by methoxyamine and N-tertbutyldimethylsilyl-N-methyltrifluoroacetamide, and analyzed by the Agilent 7890B/5977B GC MS system with a DB-5MS column (30 m × 0.25 mm × 0.25 μm film). Mass spectra were collected from 80–600 m/z under selective ion monitoring mode. The data was analyzed by Agilent MassHunter Quantitative Analysis Software and natural abundance was corrected by ISOCOR software. LC MS used a Shimadzu LC Nexera X2 UHPLC coupled with a QTRAP 5500 LC MS/MS (AB Sciex). An ACQUITY UPLC BEH Amide analytic column (2.1 X 50 mm, 1.7 μm, Waters) was used for chromatographic separation. Each metabolite was tuned with standards for optimal transitions. The extracted MRM peaks were integrated using MultiQuant 3.0.2 software (AB Sciex). **Table S1** lists the detailed parameters for the measured metabolites.

Animals

WT male C57 B6/J mice at 6 weeks were purchased from Jackson laboratory. Regular amino acid diet and high proline diet were customized at Envigo (**Table S2**). The diet and animal weight were weighed weekly to calculate food intake and change of body weight. After being fed for two weeks, animals received a single intraperitoneal injection of sodium iodate (35 mg/kg) or PBS. Mouse experiments were performed in accordance with the National Institutes of Health guidelines and the protocol was approved by the Institutional Animal Care and Use Committee of West Virginia University.

***In vivo* infusion of ^{13}C proline**

Arterial and venous catheters were surgically implanted into the jugular veins and carotid artery of animals with vascular access button on the back 1 week prior to infusions (25). After fasting for 6 hrs in the morning, mice were constantly infused with ^{13}C proline through the jugular vein for 4 hrs using the Pump 11 Elite Infuse pump and mouse infusion setup (Instech Laboratories). The mouse infusion setup included a tether and swivel system that enabled free movement of the infused mice in the cage. 10 μl of blood was collected from an arterial catheter. At the end of infusion, the mouse was euthanized by cervical dislocation. Retinas and RPE/choroid were quickly dissected with cut and pick method (31) and snap frozen in liquid nitrogen for metabolite analysis.

Electroretinography (ERG)

Mice were dark-adapted overnight before ERG using the UTAS Visual Diagnostic System with BigShot Ganzfeld with UBA-4200 amplifier and interface (LKC Technologies, Gaithersburg, MD, USA) (71). Mice were anesthetized with isoflurane and eyes were dilated with 2.5 % phenylephrine (Paragon) and 1% tropicamide (Sandoz). Scotopic ERG recordings were elicited using flashes of LED white light at increasing flash intensities (-32, -24,-16, -12, -4, 0 dB) under red light. Responses were averaged at each light intensity. Values were normalized to the baseline and each eye was evaluated separately to determine the a-wave and b-wave amplitudes.

Statistics

The significance of differences between means was determined by unpaired two-tailed t tests or analysis of variance with an appropriate post hoc test. $p < 0.05$ was considered to be significant using Graphpad Prism 7.

Acknowledgments: We thank Allison Grenell for assistance in animal ERG.

Conflict of Interest: None declared.

Author Contributions: Conceptualization, J.D; Investigation, M.Y., A. L. E., Y.W., S.Z., A.H., D.L., R.Z., J.H., M.D. C.Z., and J.D.; Writing, M.Y., J.R.C., and J.D.; Funding Acquisition, J.R.C., and J.D; Supervision, J.R.C., and J.D.

Footnotes

This work was supported by NIH Grants EY026030 (to J.R.C. and J.D.), the Brightfocus Foundation (to J.D. and J.R.C.), Retina Research Foundation (J.D.), and an unrestricted grant from Research to Prevent Blindness (J.R.C.).

References

1. Du, J., Yanagida, A., Knight, K., Engel, A. L., Vo, A. H., Jankowski, C., Sadilek, M., Tran, V. T., Manson, M. A., Ramakrishnan, A., Hurley, J. B., and Chao, J. R. (2016) Reductive carboxylation is a major metabolic pathway in the retinal pigment epithelium. *Proceedings of the National Academy of Sciences of the United States of America* **113**, 14710-14715
2. Chao, J. R., Knight, K., Engel, A. L., Jankowski, C., Wang, Y., Manson, M. A., Gu, H., Djukovic, D., Raftery, D., Hurley, J. B., and Du, J. (2017) Human retinal pigment epithelial cells prefer proline as a nutrient and transport metabolic intermediates to the retinal side. *The Journal of biological chemistry* **292**, 12895-12905
3. Phang, J. M., Liu, W., and Zabirnyk, O. (2010) Proline metabolism and microenvironmental stress. *Annual review of nutrition* **30**, 441-463
4. Phang, J. M., Donald, S. P., Pandhare, J., and Liu, Y. (2008) The metabolism of proline, a stress substrate, modulates carcinogenic pathways. *Amino acids* **35**, 681-690
5. Liang, X., Zhang, L., Natarajan, S. K., and Becker, D. F. (2013) Proline mechanisms of stress survival. *Antioxidants & redox signaling* **19**, 998-1011
6. Ben Rejeb, K., Abdelly, C., and Savoure, A. (2014) How reactive oxygen species and proline face stress together. *Plant physiology and biochemistry : PPB* **80**, 278-284
7. Zhang, L., and Becker, D. F. (2015) Connecting proline metabolism and signaling pathways in plant senescence. *Frontiers in plant science* **6**, 552
8. Hancock, C. N., Liu, W., Alvord, W. G., and Phang, J. M. (2016) Co-regulation of mitochondrial respiration by proline dehydrogenase/oxidase and succinate. *Amino acids* **48**, 859-872
9. McDonald, A. E., Pichaud, N., and Darveau, C. A. (2018) "Alternative" fuels contributing to mitochondrial electron transport: Importance of non-classical pathways in the diversity of animal metabolism. *Comparative biochemistry and physiology. Part B, Biochemistry & molecular biology* **224**, 185-194
10. Edwards, C., Canfield, J., Copes, N., Brito, A., Rehan, M., Lipps, D., Brunquell, J., Westerheide, S. D., and Bradshaw, P. C. (2015) Mechanisms of amino acid-mediated lifespan extension in Caenorhabditis elegans. *BMC genetics* **16**, 8
11. Schroeder, E. A., and Shadel, G. S. (2012) Alternative mitochondrial fuel extends life span. *Cell metabolism* **15**, 417-418
12. Zarse, K., Schmeisser, S., Groth, M., Priebe, S., Beuster, G., Kuhlow, D., Guthke, R., Platzer, M., Kahn, C. R., and Ristow, M. (2012) Impaired insulin/IGF1 signaling extends life span by promoting mitochondrial L-proline catabolism to induce a transient ROS signal. *Cell metabolism* **15**, 451-465

13. Wolthuis, D. F., van Asbeck, E., Mohamed, M., Gardeitchik, T., Lim-Melia, E. R., Wevers, R. A., and Morava, E. (2014) Cutis laxa, fat pads and retinopathy due to ALDH18A1 mutation and review of the literature. *European journal of paediatric neurology : EJPN : official journal of the European Paediatric Neurology Society* **18**, 511-515
14. O'Donnell, J. J., Sandman, R. P., and Martin, S. R. (1978) Gyrate atrophy of the retina: inborn error of L-ornithin:2-oxoacid aminotransferase. *Science* **200**, 200-201
15. Wang, T., Lawler, A. M., Steel, G., Sipila, I., Milam, A. H., and Valle, D. (1995) Mice lacking ornithine-delta-aminotransferase have paradoxical neonatal hypoornithinaemia and retinal degeneration. *Nature genetics* **11**, 185-190
16. Wang, T., Milam, A. H., Steel, G., and Valle, D. (1996) A mouse model of gyrate atrophy of the choroid and retina. Early retinal pigment epithelium damage and progressive retinal degeneration. *The Journal of clinical investigation* **97**, 2753-2762
17. Hu, C. A., Lin, W. W., Obie, C., and Valle, D. (1999) Molecular enzymology of mammalian Delta1-pyrroline-5-carboxylate synthase. Alternative splice donor utilization generates isoforms with different sensitivity to ornithine inhibition. *The Journal of biological chemistry* **274**, 6754-6762
18. Ueda, M., Masu, Y., Ando, A., Maeda, H., Del Monte, M. A., Uyama, M., and Ito, S. (1998) Prevention of ornithine cytotoxicity by proline in human retinal pigment epithelial cells. *Investigative ophthalmology & visual science* **39**, 820-827
19. Ando, A., Ueda, M., Uyama, M., Masu, Y., Okumura, T., and Ito, S. (2000) Heterogeneity in ornithine cytotoxicity of bovine retinal pigment epithelial cells in primary culture. *Experimental eye research* **70**, 89-96
20. Bennis, A., Gorgels, T. G., Ten Brink, J. B., van der Spek, P. J., Bossers, K., Heine, V. M., and Bergen, A. A. (2015) Comparison of Mouse and Human Retinal Pigment Epithelium Gene Expression Profiles: Potential Implications for Age-Related Macular Degeneration. *PloS one* **10**, e0141597
21. Liao, J. L., Yu, J., Huang, K., Hu, J., Diemer, T., Ma, Z., Dvash, T., Yang, X. J., Travis, G. H., Williams, D. S., Bok, D., and Fan, G. (2010) Molecular signature of primary retinal pigment epithelium and stem-cell-derived RPE cells. *Human molecular genetics* **19**, 4229-4238
22. Strunnikova, N. V., Maminishkis, A., Barb, J. J., Wang, F., Zhi, C., Sergeev, Y., Chen, W., Edwards, A. O., Stambolian, D., Abecasis, G., Swaroop, A., Munson, P. J., and Miller, S. S. (2010) Transcriptome analysis and molecular signature of human retinal pigment epithelium. *Human molecular genetics* **19**, 2468-2486
23. Gao, X. R., Huang, H., and Kim, H. (2019) Genome-wide association analyses identify 139 loci associated with macular thickness in the UK Biobank cohort. *Human molecular genetics* **28**, 1162-1172
24. Du, J., Cleghorn, W., Contreras, L., Linton, J. D., Chan, G. C., Chertov, A. O., Saheki, T., Govindaraju, V., Sadilek, M., Satrustegui, J., and Hurley, J. B. (2013) Cytosolic reducing power preserves glutamate in retina. *Proceedings of the National Academy of Sciences of the United States of America* **110**, 18501-18506
25. Ayala, J. E., Bracy, D. P., Malabanan, C., James, F. D., Ansari, T., Fueger, P. T., McGuinness, O. P., and Wasserman, D. H. (2011) Hyperinsulinemic-euglycemic clamps in conscious, unrestrained mice. *Journal of visualized experiments : JoVE*
26. Davidson, S. M., Papagiannakopoulos, T., Olenchock, B. A., Heyman, J. E., Keibler, M. A., Luengo, A., Bauer, M. R., Jha, A. K., O'Brien, J. P., Pierce, K. A., Gui, D. Y., Sullivan, L. B., Wasylenko, T. M., Subbaraj, L., Chin, C. R., Stephanopolous, G., Mott, B. T., Jacks, T., Clish, C. B., and Vander Heiden, M. G. (2016) Environment Impacts the Metabolic Dependencies of Ras-Driven Non-Small Cell Lung Cancer. *Cell metabolism* **23**, 517-528
27. Krishnan, N., Dickman, M. B., and Becker, D. F. (2008) Proline modulates the intracellular redox environment and protects mammalian cells against oxidative stress. *Free radical biology & medicine* **44**, 671-681

28. Seiler, N. (2000) Ornithine aminotransferase, a potential target for the treatment of hyperammonemias. *Current drug targets* **1**, 119-153
29. Adachi, R., Okada, K., Skene, R., Ogawa, K., Miwa, M., Tsuchinaga, K., Ohkubo, S., Henta, T., and Kawamoto, T. (2017) Discovery of a novel prolyl-tRNA synthetase inhibitor and elucidation of its binding mode to the ATP site in complex with l-proline. *Biochemical and biophysical research communications* **488**, 393-399
30. Xiong, G., Deng, L., Zhu, J., Rychahou, P. G., and Xu, R. (2014) Prolyl-4-hydroxylase alpha subunit 2 promotes breast cancer progression and metastasis by regulating collagen deposition. *BMC cancer* **14**, 1
31. Zhu, S., Yam, M., Wang, Y., Linton, J. D., Grenell, A., Hurley, J. B., and Du, J. (2018) Impact of euthanasia, dissection and postmortem delay on metabolic profile in mouse retina and RPE/choroid. *Experimental eye research* **174**, 113-120
32. Xu, L., Kong, L., Wang, J., and Ash, J. D. (2018) Stimulation of AMPK prevents degeneration of photoreceptors and the retinal pigment epithelium. *Proceedings of the National Academy of Sciences of the United States of America* **115**, 10475-10480
33. Chowers, G., Cohen, M., Marks-Ohana, D., Stika, S., Eijzenberg, A., Banin, E., and Obolensky, A. (2017) Course of Sodium Iodate-Induced Retinal Degeneration in Albino and Pigmented Mice. *Investigative ophthalmology & visual science* **58**, 2239-2249
34. Eswarappa, S. M., Potdar, A. A., Sahoo, S., Sankar, S., and Fox, P. L. (2018) Metabolic origin of the fused aminoacyl tRNA synthetase, glutamyl-prolyl tRNA synthetase. *The Journal of biological chemistry*
35. Nita, M., Strzalka-Mrozik, B., Grzybowski, A., Mazurek, U., and Romaniuk, W. (2014) Age-related macular degeneration and changes in the extracellular matrix. *Medical science monitor : international medical journal of experimental and clinical research* **20**, 1003-1016
36. Kigasawa, K., Ishikawa, H., Obazawa, H., Minamoto, T., Nagai, Y., and Tanaka, Y. (1998) Collagen production by cultured human retinal pigment epithelial cells. *The Tokai journal of experimental and clinical medicine* **23**, 147-151
37. Li, W., Stramm, L. E., Aguirre, G. D., and Rockey, J. H. (1984) Extracellular matrix production by cat retinal pigment epithelium in vitro: characterization of type IV collagen synthesis. *Experimental eye research* **38**, 291-304
38. Hirata, A., and Feeney-Burns, L. (1992) Autoradiographic studies of aged primate macular retinal pigment epithelium. *Investigative ophthalmology & visual science* **33**, 2079-2090
39. Hillenkamp, J., Hussain, A. A., Jackson, T. L., Cunningham, J. R., and Marshall, J. (2004) The influence of path length and matrix components on ageing characteristics of transport between the choroid and the outer retina. *Investigative ophthalmology & visual science* **45**, 1493-1498
40. Fisher, C. R., and Ferrington, D. A. (2018) Perspective on AMD Pathobiology: A Bioenergetic Crisis in the RPE. *Investigative ophthalmology & visual science* **59**, AMD41-AMD47
41. Bursell, E., Billing, K. J., Hargrove, J. W., McCabe, C. T., and Slack, E. (1973) The supply of substrates to the flight muscle of tsetse flies. *Transactions of the Royal Society of Tropical Medicine and Hygiene* **67**, 296
42. Liu, L. K., Becker, D. F., and Tanner, J. J. (2017) Structure, function, and mechanism of proline utilization A (PutA). *Archives of biochemistry and biophysics* **632**, 142-157
43. Sinha, T., Makia, M., Du, J., Naash, M. I., and Al-Ubaidi, M. R. (2018) Flavin homeostasis in the mouse retina during aging and degeneration. *The Journal of nutritional biochemistry* **62**, 123-133
44. Elia, I., Broekaert, D., Christen, S., Boon, R., Radaelli, E., Orth, M. F., Verfaillie, C., Grunewald, T. G. P., and Fendt, S. M. (2017) Proline metabolism supports metastasis formation and could be inhibited to selectively target metastasizing cancer cells. *Nat Commun* **8**, 15267
45. Agathocleous, M., and Harris, W. A. (2013) Metabolism in physiological cell proliferation and differentiation. *Trends in cell biology* **23**, 484-492

46. Zheng, X., Boyer, L., Jin, M., Mertens, J., Kim, Y., Ma, L., Hamm, M., Gage, F. H., and Hunter, T. (2016) Metabolic reprogramming during neuronal differentiation from aerobic glycolysis to neuronal oxidative phosphorylation. *eLife* **5**
47. Iacovelli, J., Rowe, G. C., Khadka, A., Diaz-Aguilar, D., Spencer, C., Arany, Z., and Saint-Geniez, M. (2016) PGC-1alpha Induces Human RPE Oxidative Metabolism and Antioxidant Capacity. *Investigative ophthalmology & visual science* **57**, 1038-1051
48. Adijanto, J., and Philp, N. J. (2014) Cultured primary human fetal retinal pigment epithelium (hfRPE) as a model for evaluating RPE metabolism. *Experimental eye research* **126**, 77-84
49. Ahmado, A., Carr, A. J., Vugler, A. A., Semo, M., Gias, C., Lawrence, J. M., Chen, L. L., Chen, F. K., Turowski, P., da Cruz, L., and Coffey, P. J. (2011) Induction of differentiation by pyruvate and DMEM in the human retinal pigment epithelium cell line ARPE-19. *Investigative ophthalmology & visual science* **52**, 7148-7159
50. Whitmore, S. S., Wagner, A. H., DeLuca, A. P., Drack, A. V., Stone, E. M., Tucker, B. A., Zeng, S., Braun, T. A., Mullins, R. F., and Scheetz, T. E. (2014) Transcriptomic analysis across nasal, temporal, and macular regions of human neural retina and RPE/choroid by RNA-Seq. *Experimental eye research* **129**, 93-106
51. Hwang, I. Y., Kwak, S., Lee, S., Kim, H., Lee, S. E., Kim, J. H., Kim, Y. A., Jeon, Y. K., Chung, D. H., Jin, X., Park, S., Jang, H., Cho, E. J., and Youn, H. D. (2016) Psat1-Dependent Fluctuations in alpha-Ketoglutarate Affect the Timing of ESC Differentiation. *Cell metabolism* **24**, 494-501
52. Gu, H., Du, J., Carnevale Neto, F., Carroll, P. A., Turner, S. J., Chiorean, E. G., Eisenman, R. N., and Raftery, D. (2015) Metabolomics method to comprehensively analyze amino acids in different domains. *The Analyst* **140**, 2726-2734
53. Hirabayashi, Y., and Furuya, S. (2008) Roles of l-serine and sphingolipid synthesis in brain development and neuronal survival. *Progress in lipid research* **47**, 188-203
54. Marmorstein, L. Y., McLaughlin, P. J., Peachey, N. S., Sasaki, T., and Marmorstein, A. D. (2007) Formation and progression of sub-retinal pigment epithelium deposits in Efemp1 mutation knock-in mice: a model for the early pathogenic course of macular degeneration. *Human molecular genetics* **16**, 2423-2432
55. Fan, J., Ye, J., Kamphorst, J. J., Shlomi, T., Thompson, C. B., and Rabinowitz, J. D. (2014) Quantitative flux analysis reveals folate-dependent NADPH production. *Nature* **510**, 298-302
56. Eswarappa, S. M., Potdar, A. A., Sahoo, S., Sankar, S., and Fox, P. L. (2018) Metabolic origin of the fused aminoacyl-tRNA synthetase, glutamyl-prolyl-tRNA synthetase. *The Journal of biological chemistry* **293**, 19148-19156
57. Ribas de Pouplana, L. (2018) Genetic code and metabolism: The perpetual waltz. *The Journal of biological chemistry* **293**, 19157-19158
58. Newman, A. M., Gallo, N. B., Hancox, L. S., Miller, N. J., Radeke, C. M., Maloney, M. A., Cooper, J. B., Hageman, G. S., Anderson, D. H., Johnson, L. V., and Radeke, M. J. (2012) Systems-level analysis of age-related macular degeneration reveals global biomarkers and phenotype-specific functional networks. *Genome medicine* **4**, 16
59. Allmann, S., Morand, P., Ebikeme, C., Gales, L., Biran, M., Hubert, J., Brennand, A., Mazet, M., Franconi, J. M., Michels, P. A., Portais, J. C., Boshart, M., and Bringaud, F. (2013) Cytosolic NADPH homeostasis in glucose-starved procyclic Trypanosoma brucei relies on malic enzyme and the pentose phosphate pathway fed by gluconeogenic flux. *The Journal of biological chemistry* **288**, 18494-18505
60. Fronk, A. H., and Vargis, E. (2016) Methods for culturing retinal pigment epithelial cells: a review of current protocols and future recommendations. *Journal of tissue engineering* **7**, 2041731416650838
61. Maminishkis, A., Chen, S., Jalickee, S., Banzon, T., Shi, G., Wang, F. E., Ehalt, T., Hammer, J. A., and Miller, S. S. (2006) Confluent monolayers of cultured human fetal retinal pigment epithelium exhibit morphology and physiology of native tissue. *Investigative ophthalmology & visual science* **47**, 3612-3624

62. Hu, J., and Bok, D. (2001) A cell culture medium that supports the differentiation of human retinal pigment epithelium into functionally polarized monolayers. *Molecular vision* **7**, 14-19
63. Radeke, M. J., Radeke, C. M., Shih, Y. H., Hu, J., Bok, D., Johnson, L. V., and Coffey, P. J. (2015) Restoration of mesenchymal retinal pigmented epithelial cells by TGFbeta pathway inhibitors: implications for age-related macular degeneration. *Genome medicine* **7**, 58
64. Hurley, J. B., Lindsay, K. J., and Du, J. (2015) Glucose, lactate, and shuttling of metabolites in vertebrate retinas. *Journal of neuroscience research* **93**, 1079-1092
65. Bui, B. V., Hu, R. G., Acosta, M. L., Donaldson, P., Vingrys, A. J., and Kalloniatis, M. (2009) Glutamate metabolic pathways and retinal function. *Journal of neurochemistry* **111**, 589-599
66. Reichenbach, A., Henke, A., Eberhardt, W., Reichelt, W., and Dettmer, D. (1992) K+ ion regulation in retina. *Canadian journal of physiology and pharmacology* **70 Suppl**, S239-247
67. Wang, J., Iacovelli, J., Spencer, C., and Saint-Geniez, M. (2014) Direct effect of sodium iodate on neurosensory retina. *Investigative ophthalmology & visual science* **55**, 1941-1953
68. Sonoda, S., Spee, C., Barron, E., Ryan, S. J., Kannan, R., and Hinton, D. R. (2009) A protocol for the culture and differentiation of highly polarized human retinal pigment epithelial cells. *Nature protocols* **4**, 662-673
69. Buchholz, D. E., Pennington, B. O., Croze, R. H., Hinman, C. R., Coffey, P. J., and Clegg, D. O. (2013) Rapid and efficient directed differentiation of human pluripotent stem cells into retinal pigmented epithelium. *Stem cells translational medicine* **2**, 384-393
70. Du, J., Linton, J. D., and Hurley, J. B. (2015) Probing Metabolism in the Intact Retina Using Stable Isotope Tracers. *Methods in enzymology* **561**, 149-170
71. Wang, Y., Grenell, A., Zhong, F., Yam, M., Hauer, A., Gregor, E., Zhu, S., Lohner, D., Zhu, J., and Du, J. (2018) Metabolic signature of the aging eye in mice. *Neurobiology of aging* **71**, 223-233

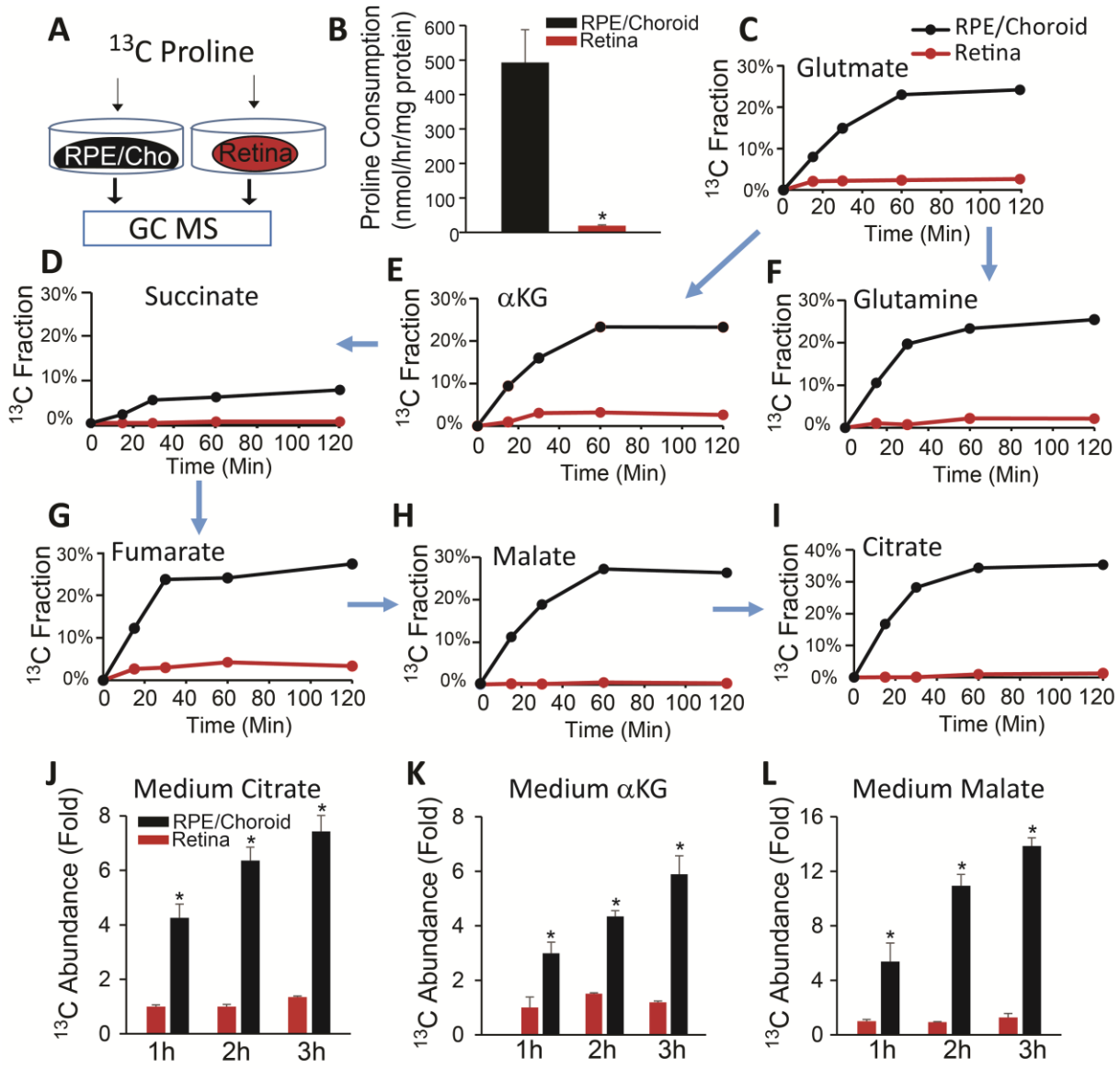

Figure 1. Mouse RPE/choroid utilizes ^{13}C proline *ex vivo*. (A) Schematic for *ex vivo* incubation of ^{13}C proline. Freshly isolated RPE/choroid or retina was incubated in 5 mM glucose and 1 mM ^{13}C proline for different time. (B-D) RPE/choroid consumes much more proline than retina and generates mitochondrial intermediates. Metabolites were analyzed by GC MS. ^{13}C fraction is the percent of labeled carbon of total isotopologues or ^{13}C labeled metabolite in the total pool. Arrows represent the direction that the carbons flow in mitochondrial krebs cycle. (J-L) Proline-derived metabolites are exported into media. ^{13}C abundance fold change was calculated from the ion intensity of labeled metabolites relative to those in retina at 1 hr. *P<0.05 vs retina. N=4.

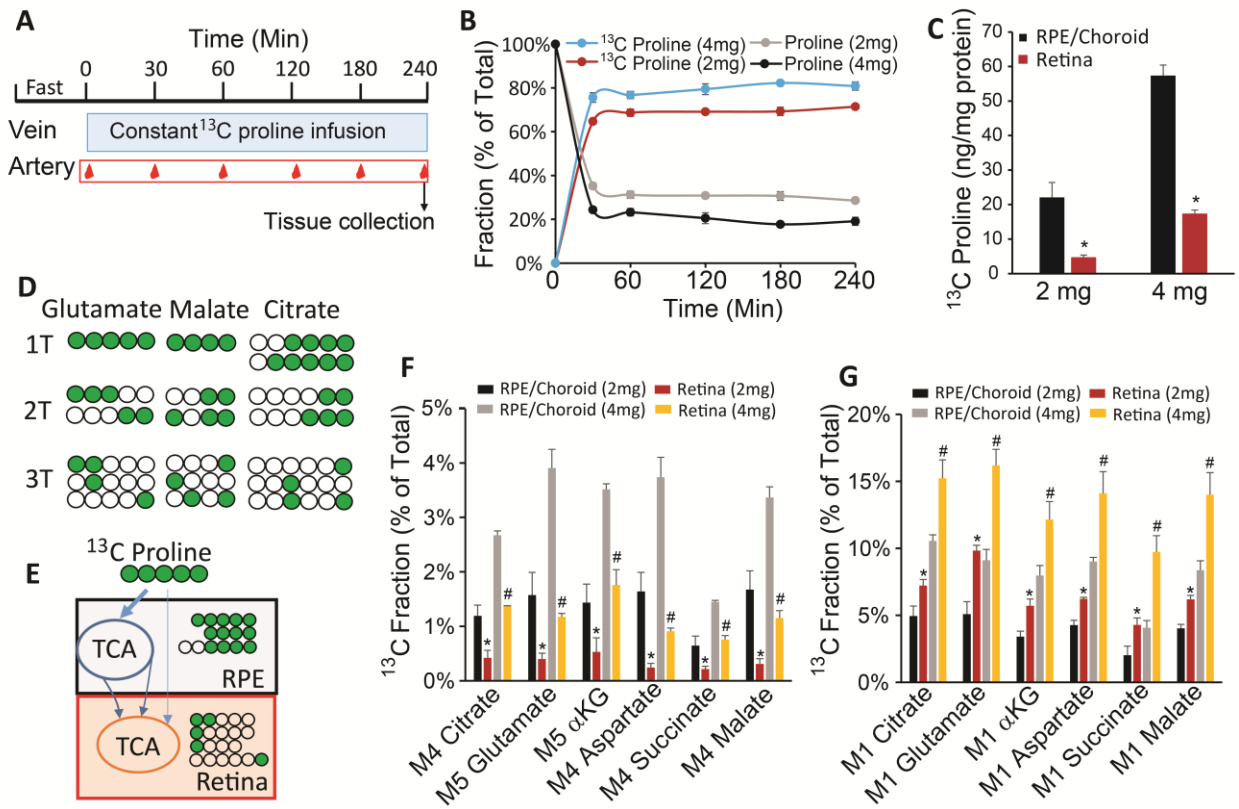

Figure 2. Proline utilization in RPE and retina *in vivo*. (A) Schematic for ^{13}C proline infusion *in vivo*. After fasting for 6 hrs, ^{13}C proline was constantly infused through a jugular catheter in free-moving mice. Blood samples were collected through an arterial catheter. (B) ^{13}C proline replaced unlabeled proline and reached steady state in the plasma after infusion. (C) RPE/choroid had more ^{13}C proline than retina. (D-E) Schematic of ^{13}C labeling pattern in RPE and retina. After entering the TCA cycle, five carbon labeled ^{13}C proline was catabolized mostly into M5/M4 metabolites in the first turn (1T) of TCA cycle, M2/M3 in 2T and M1 in 3T. When RPE used proline initially and exported the intermediates, RPE should have more M5/M4 and retina should have more M1. (F-G) M5/M4 metabolites were increased while M1 metabolites were decreased in the RPE comparable to the retina. N=4. *P <0.05 vs retinas with 2 mg/kg/min of ^{13}C proline and $^{\#}$P<0.05 vs retinas with 4 mg/kg/min of ^{13}C proline.

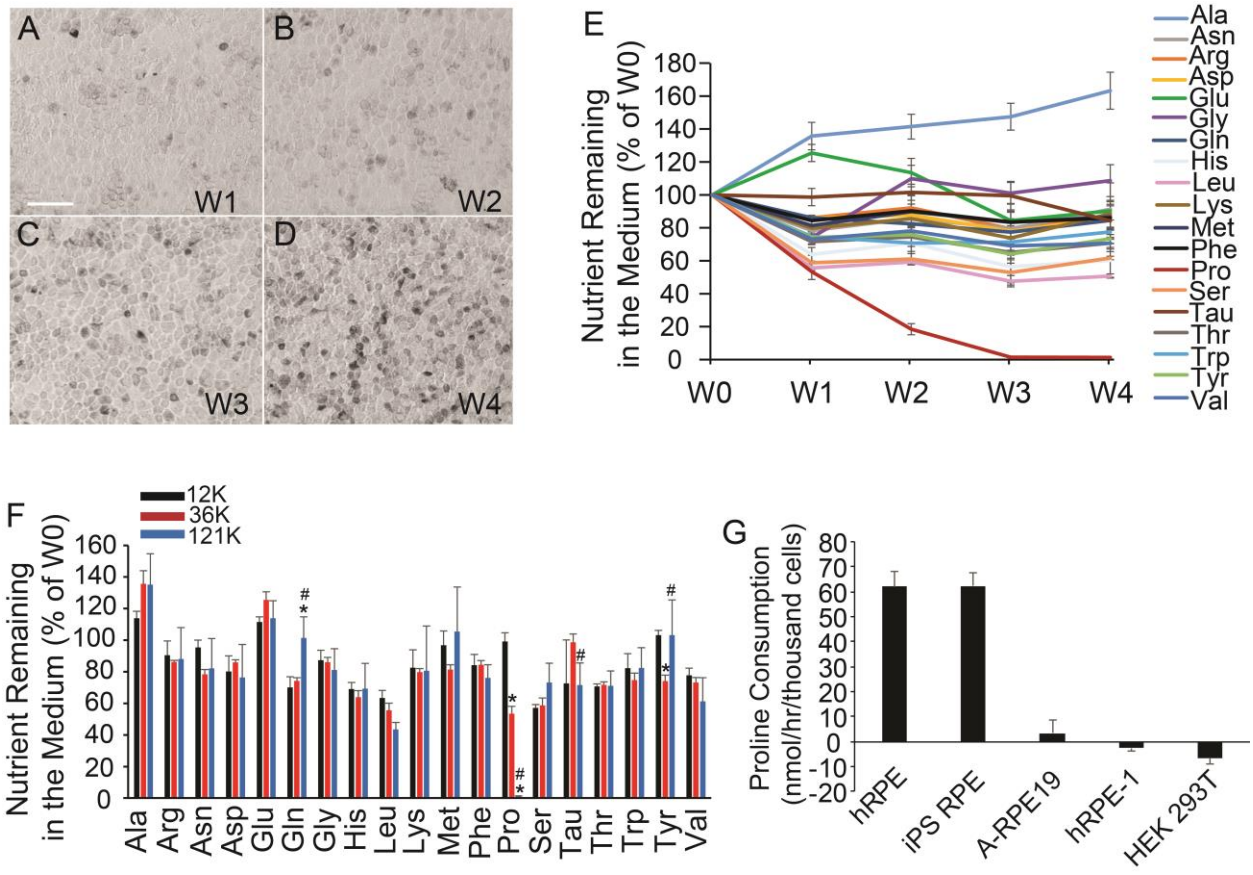

Figure 3. RPE switches to utilize proline during maturation. (A-D) Human RPE matured after 3-4 weeks of culture. RPE cells showed typical cobble stone morphology and are pigmented under bright field microscopy. Scale=100 μm (E) Nutrient consumption at different weeks of culture. For each week of culture, media was collected for GC-MS 24hrs after being changed. Y axis represents the amount of nutrient left in the media relative to fresh media. (F) RPE cells were plated at different densities and grown for a week. Nutrients remaining in the media 24 hrs after medium change were analyzed by GC MS. K, thousands/per well. (G) Proline consumption in RPE cells and cell lines. N=4. *P <0.05 vs RPE cells plated at 12K and $^{\#}$P<0.05 vs RPE cells plated at 36K.

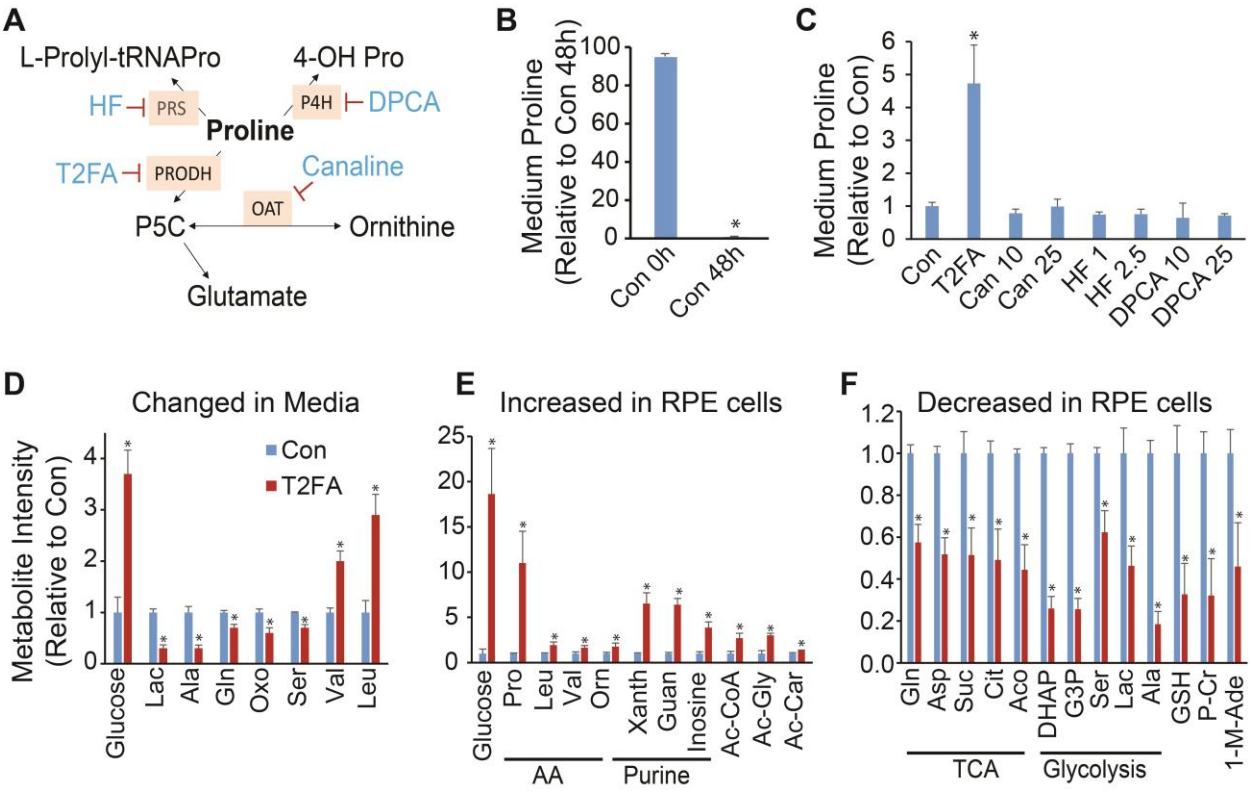

Figure 4. Inhibition of proline catabolism partially blocked proline consumption and impaired glucose metabolism. (A) Schematic for inhibitors and pathways in proline metabolism. (B) RPE consumed most proline in media after culture for 48 hrs. (C) T2FA partially blocked proline consumption. Inhibitors at different concentrations were incubated for 48 hrs. Con was RPE media with DMSO after 48-hr culture. T2FA concentration was 5 mM and other inhibitors were at different concentration as labeled in μM. (D-E) Changes of metabolites in the media or cells were measured by LC MS. N=4. *P <0.05 vs Con without T2FA at 48 hrs. Lac, lactate; Oxo, 5-oxoproline; Xanth, xanthine; Guan, guanine; Ac, acetyl-; Ac-Car, acetyl-carnitine; Suc, succinate; Cit, citrate; Aco, aconitate; P-Cr, phosphocreatine; GSH, glutathione; 1-M-Ade, 1-methyl-adenosine.

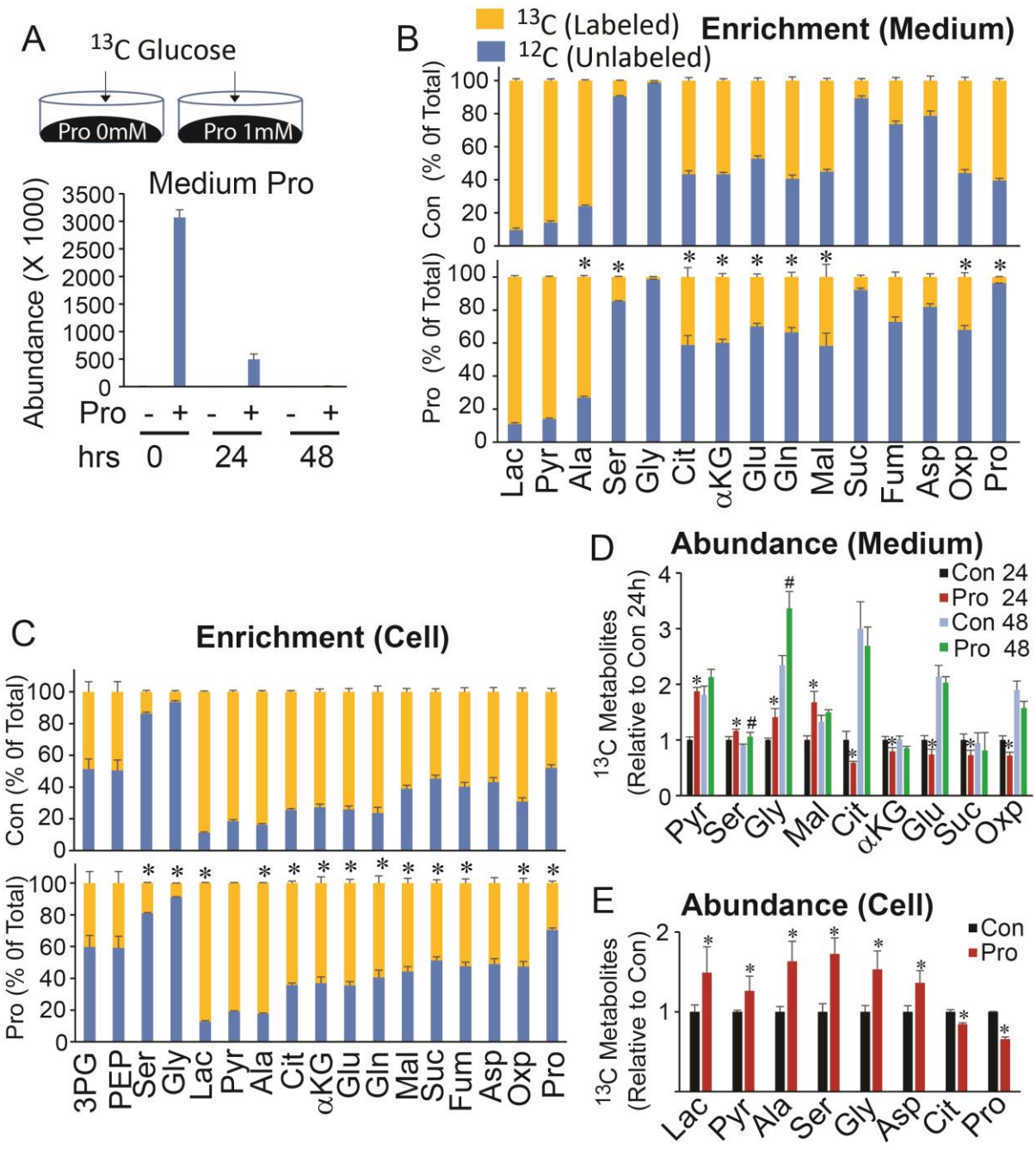

Figure 5. Proline regulates glucose metabolism and stimulates synthesis of serine and glycine. (A) Schematic for ^{13}C glucose incubation in matured hRPE cells cultured with or without proline in DMEM. (B) Proline decreased the ^{13}C fraction (^{13}C enrichment) of mitochondrial intermediates in the media after 24 hrs of culture. Top panel was medium without proline and bottom was the medium with 1 mM proline. (C) The ^{13}C fraction of mitochondrial intermediates were decreased but serine and glycine were increased by proline. (D-E) Proline regulated the levels of ^{13}C labeled metabolites from ^{13}C glucose in media and RPE cells. Metabolites were measured by GC MS. N=4. *P <0.05 vs Con without proline or Con at 24 hrs. $^{\#}P<0.05$ vs Con at 48 hrs. Lac, lactate; Pyr, pyruvate; 3PG, 3-Phosphoglyceric acid; PEP, phosphoenolpyruvate; Oxp, 5-oxoproline.

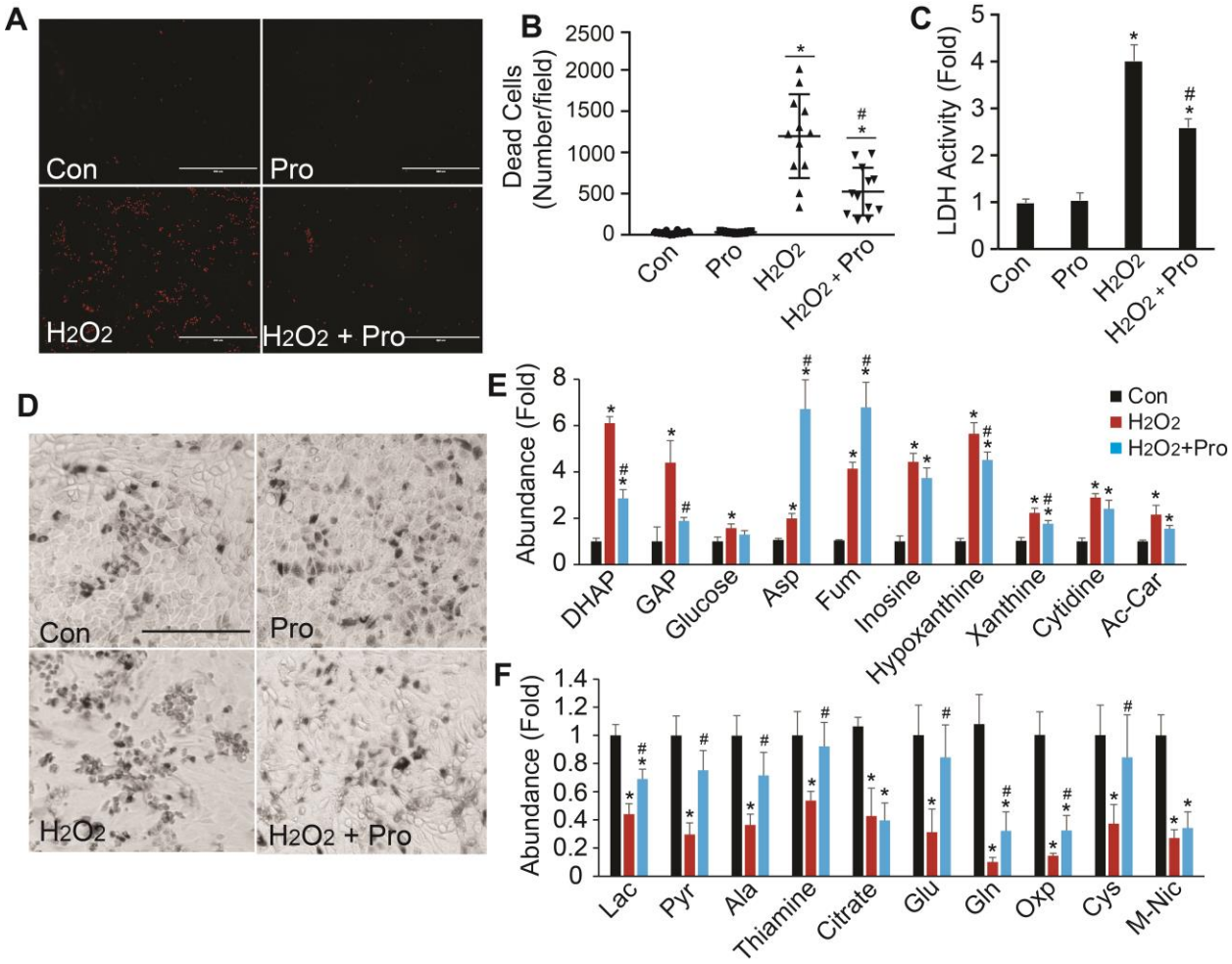

Figure 6. Proline protects oxidative damage in RPE cells. (A) Representative images for EthD staining. RPE cells were stained with EthD and red fluorescent cells were dead cells. Scale=400 μm. (B) Quantitation of dead cells stained by EthD by image J. *P <0.05 vs Con without proline and #P <0.05 vs cells with H_2O_2. N=12. (C) Proline reduced the LDH activity by H_2O_2 in the media. LDH activity was the fold of change relative to Con without proline. *P <0.05 vs Con without proline and #P <0.05 vs cells with H_2O_2. N=4. (D) Proline improved cell morphology impaired by H_2O_2. Scale=400 μm. (E-F) Significantly changed metabolites in RPE media (E) and cells (F) with proline after H_2O_2 treatment for 24 hrs. N=4. *P <0.05 vs Con without proline and #P <0.05 vs cells with H_2O_2. Ac-Car, aceyl-carnitine; Oxo, 5-oxoproline; M-Nic, methyl-nicotinamide.

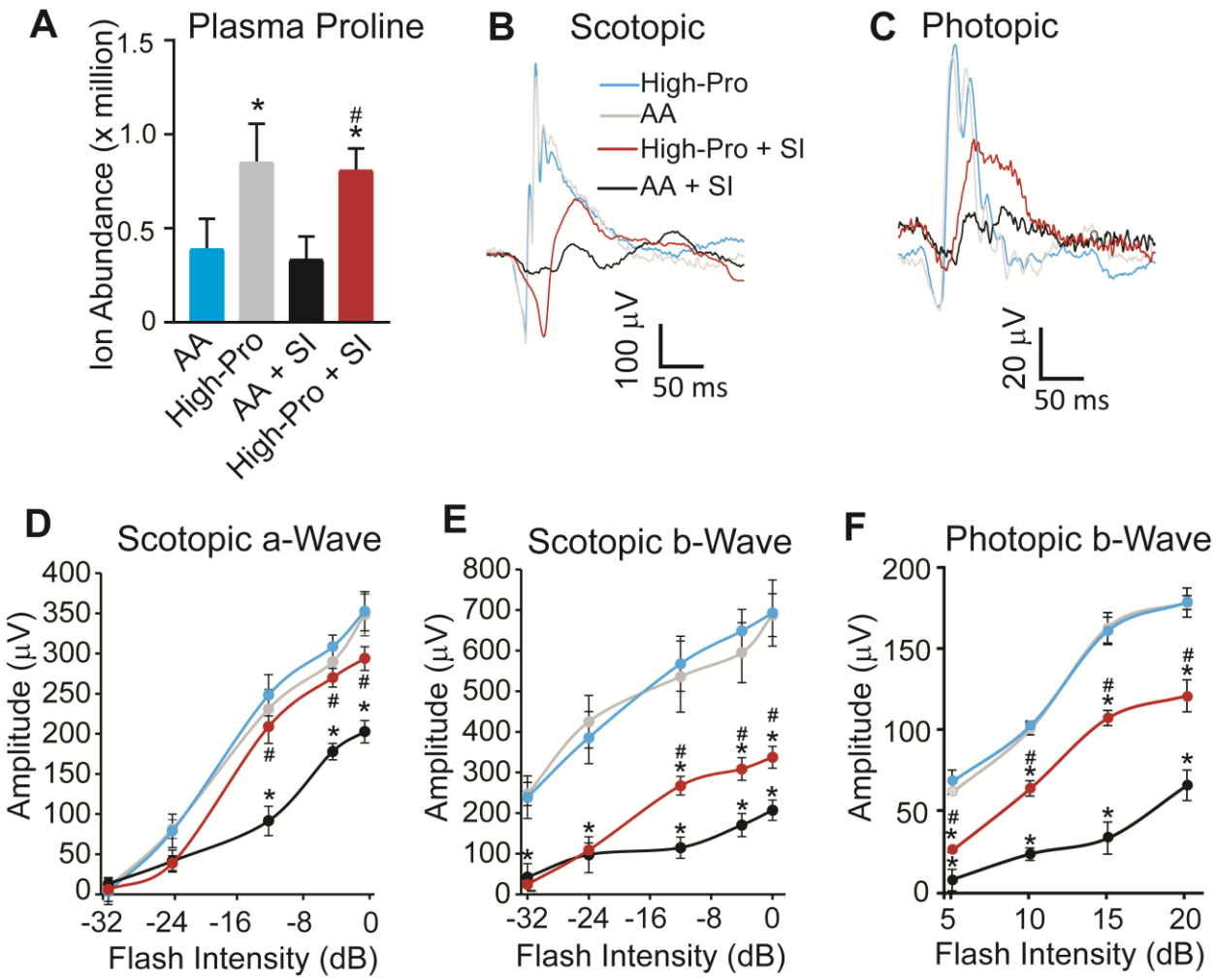

Figure 7. Proline improves visual function induced by oxidative damage. (A) High-proline diet doubled plasma proline in mice with or without sodium iodate (SI). N=6. *P <0.05 vs AA (amino acid) diet alone and #P <0.05 vs AA diet with SI. (B-F) High-Proline diet improved ERGs with SI. (B) was a representative raw trace of scotopic response at -12 dB and C was a raw trace of photopic response at 10 dB. N=10. *P <0.05 vs AA diet alone and #P <0.05 vs AA diet with SI.

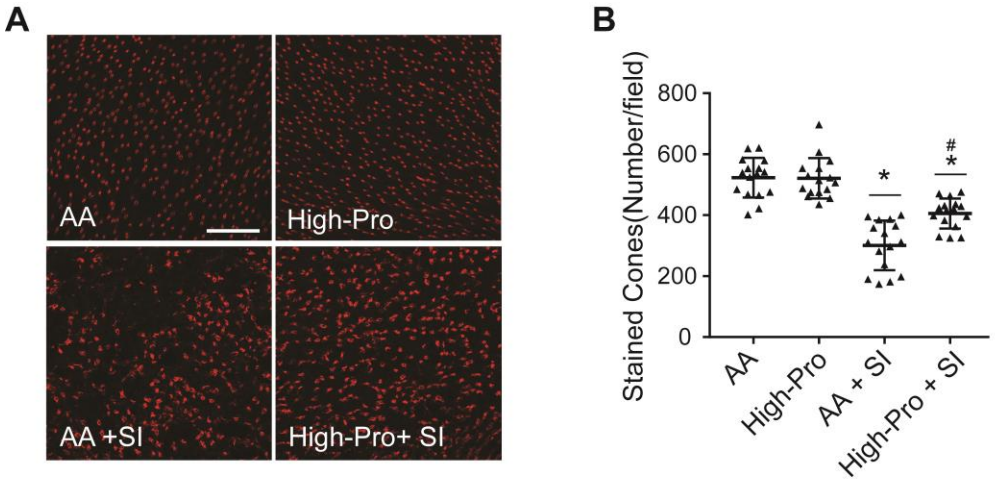

Figure 8. Proline reduces SI-induced photoreceptor cell death. (A) Representative images of flat mount staining with PNA. Scale = 10 μm. (B) was the quantification of PNA staining with Image J to count stained cone photoreceptors in each field. N=16 from 4 animals in each group. P <0.05 vs AA diet alone and $^{\#}$P <0.05 vs AA diet with SI.

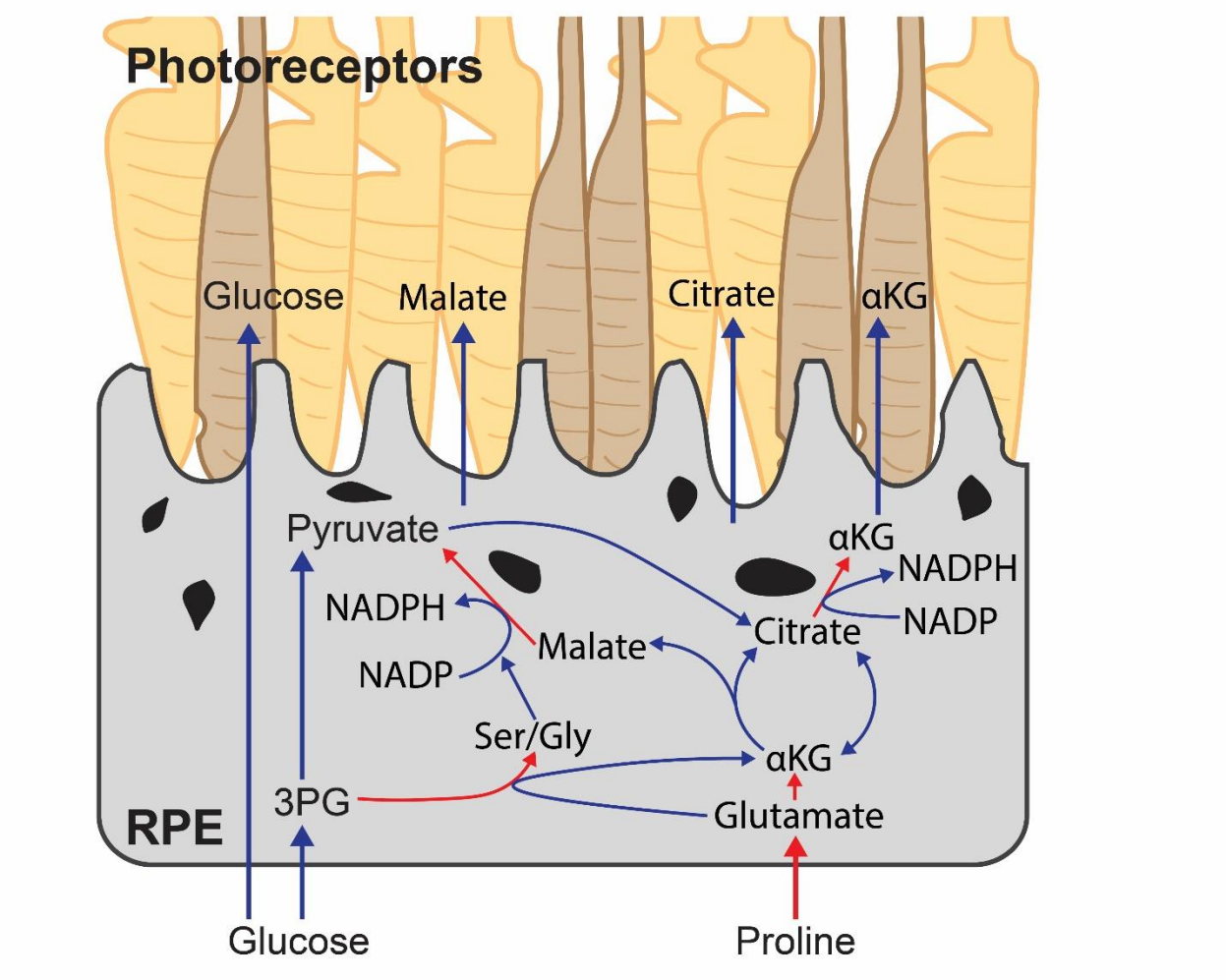

Figure 9. A model of proline-mediated metabolic communication between RPE and photoreceptors. RPE cells utilizes proline in RPE to generate mitochondrial intermediates through TCA cycle and NADPH. These intermediates export RPE to be used by photoreceptors. The activation of NADPH-generation pathways by proline protects RPE from oxidative damage. Additionally, the utilization of proline in RPE may spare the oxidation of glucose which is a major nutrient in photoreceptors. Red arrows represents pathways in proline utilization.